Available online at www.sciencedirect.com
SCIENCE DIRECT®
Journal of Inorganic Biochemistry 98 (2004) 1361–1366
Journal of Inorganic Biochemistry
www.elsevier.com/locate/jinorgbio

Synthesis, X-ray crystal structure, anti-fungal and anti-cancer activity of $[Ag_2(NH_3)_2(salH)_2]$ ($salH_2$ = salicylic acid)

Barry Coyle [a], Malachy McCann [a,*], Kevin Kavanagh [b], Michael Devereux [c], Vickie McKee [d], Nijhuma Kayal [d], Denise Egan [e], Carol Deegan [e], Gregory J. Finn [f]

[a] Chemistry Department, National University of Ireland Maynooth, Maynooth, Co. Kildare, Ireland
[b] Biology Department, National University of Ireland Maynooth, Maynooth, Co. Kildare, Ireland
[c] Dublin Institute of Technology, Cathal Brugha Street, Dublin, Ireland
[d] Chemistry Department, Loughborough University, Loughborough, Leics., LE11 3TU, UK
[e] Department of Applied Science, Institute of Technology, Tallaght, Dublin 24, Ireland
[f] Cancer Research Program, Beth Israel Deaconess Medical Centre, Harvard Institutes of Medicine, Harvard Medical School, Boston, MA, USA

Received 21 January 2004; received in revised form 1 April 2004; accepted 26 April 2004
Available online 15 June 2004

Abstract

$[Ag_2(NH_3)_2(salH)_2]$ ($salH_2$ = salicylic acid) was synthesised from salicylic acid and Ag_2O in concentrated aqueous NH_3 and the dimeric Ag(I) complex was characterised using X-ray crystallography. The complex is centrosymmetric with each metal coordinated to a salicylate carboxylate oxygen and to an ammonia nitrogen atom in an almost linear fashion. The two $[Ag(NH_3)(salH)]$ units in the complex are linked by an Ag–Ag bond. Whilst metal-free $salH_2$ did not prevent the growth of the fungal pathogen *Candida albicans* $[Ag_2(NH_3)_2(salH)_2]$, $[Ag_2(salH)_2]$ and some simple Ag(I) salts greatly inhibited cell reproduction. $SalH_2$, $[Ag_2(NH_3)_2(salH)_2]$ $[Ag_2(salH)_2]$ and $AgClO_4$ produced a dose-dependent cytotoxic response against the three human derived cancer cell lines, Cal-27, Hep-G2 and A-498, with the Ag(I)-containing reagents being the most effective.

Keywords: Silver(I); Salicylate; X-ray structure; Anti-fungal; Anti-cancer

1. Introduction

In our efforts to develop new metal-based drugs for inhibiting the growth of the fungal pathogen *Candida albicans*, and also for deterring the proliferation of mammalian cancer cells, the most effective metal complex to emerge to date is the Ag(I) complex $[Ag(phendio)_2]ClO_4$ (phendio = 1,10-phenanthroline-5,6-dione) [1]. The complex has a minimum inhibitory concentration (MIC) against *C. albicans* of 0.5 $\mu g\,cm^{-3}$ (0.3 μM) and tests on cultured human cancer cells produced an IC_{50} (the concentration that inhibited growth by 50%) value of 0.025 $\mu g\,cm^{-3}$ (0.40 μM). These findings for the Ag(I) complexes were a marked improvement on values obtained using other transition metals complexed by phendio or 1,10-phenanthroline [1–3] and have prompted investigations into the preparation, characterisation and testing of other Ag(I) complexes. The present paper details the synthesis, X-ray crystal structure and biological activity of the dimeric Ag(I) complex $[Ag_2(NH_3)_2(salH)_2]$ ($salH_2$ = salicylic acid).

2. Results and discussion

The method used for preparing $[Ag_2(NH_3)_2(salH)_2]$ was quite similar to that employed for the preparation of the known non-amine analogue $[Ag_2(salH)_2]$ [4–6]. $[Ag_2(NH_3)_2(salH)_2]$ was obtained from a suspension of Ag_2O in water to which was added concentrated aqueous NH_3 followed by salicylic acid ($salH_2$). On the other hand, $[Ag_2(salH)_2]$ was prepared in an 80:20 ethanol:water solvent mixture to which was added $salH_2$,

* Corresponding author. Tel.: +353-1-7083767; fax: 353-1-7083815.
E-mail address: mmcann@may.ie (M. McCann).

0162-0134/$ - see front matter © 2004 Elsevier Inc. All rights reserved.
doi:10.1016/j.jinorgbio.2004.04.016

$AgNO_3$ and concentrated aqueous NH_3. The X-ray crystal structure of $[Ag_2(NH_3)_2(salH)_2]$ is shown in Fig. 1 and selected bond lengths and angles are given in Table 1. The complex is dimeric, centrosymmetric and close to planar. Each metal is coordinated to a salicylate carboxylate oxygen (Ag–O = 2.170 Å) and to an ammonia nitrogen atom in an almost linear fashion {O(3)–Ag–N(1) = 175.37(5)°}. A similar monodentate carboxylate coordination has been reported for the polymeric Ag(I) salicylate complex $[Ag(\mu_3\text{-hmt})(salH)]\cdot H_2O$ (hmt = hexamethylenetetramine) [7]. The Ag–O distance in $[Ag_2(NH_3)_2(salH)_2]$ is shorter than those in the *syn–syn* bis(carboxylate-bridged) dimer $[Ag_2(salH)_2]$ (2.181, 2.202 Å) [5,6]. In $[Ag_2(NH_3)_2(salH)_2]$, an almost linear N–Ag–O geometry is completed by coordination of an ammonia molecule (Ag–N = 2.137 Å).

In $[Ag_2(NH_3)_2(salH)_2]$, the two $[Ag(NH_3)(salH)]$ units are linked by an Ag–Ag bonding interaction, supported by hydrogen-bonding between the coordinated O atom of one unit and an ammonia hydrogen atom of the other. The essentially planar conformation is the result of stabilisation due to intramolecular hydrogen-bonding interactions between the *ortho*-substituted phenol and the uncoordinated carboxylate oxygen. In essence, the two monomers aggregate "head-to-tail" to allow for this hydrogen-bonding. Such hydrogen-bonding interactions have been implicated in the formation of some complexes exhibiting auriophilicity [8]. In contrast to the structure of $[Ag_2(NH_3)_2(salH)_2]$, the silver(I) benzoates with no *ortho*-hydroxyl substituents deviate markedly from planarity [9]. The Ag–Ag bond (3.069 Å) in $[Ag_2(NH_3)_2(salH)_2]$ is slightly longer than that found in $[Ag_2(salH)_2]$ (2.855 Å) implying that the ligand architecture of the *syn–syn* bridged dimers in the latter species facilitates a closer approach of the silver ions [5,6]. However, the Ag–Ag distance in $[Ag_2(NH_3)_2(salH)_2]$ is still indicative of an Ag–Ag argentophilic interaction when compared to a value of 2.89 Å for the interatomic distance in metallic silver [10]. It has been speculated that such an attractive interaction between the Ag(I) d^{10} cations is due to hybridisation of the metal 4d orbital with the higher energy 5s and 5p orbitals, which converts the closed-shell repulsion into a weak attractive interaction [11–13]. The ^1H NMR spectrum of $[Ag_2(NH_3)_2(salH)_2]$ in DMSO indicates that no ligand exchange of the complex with DMSO takes place.

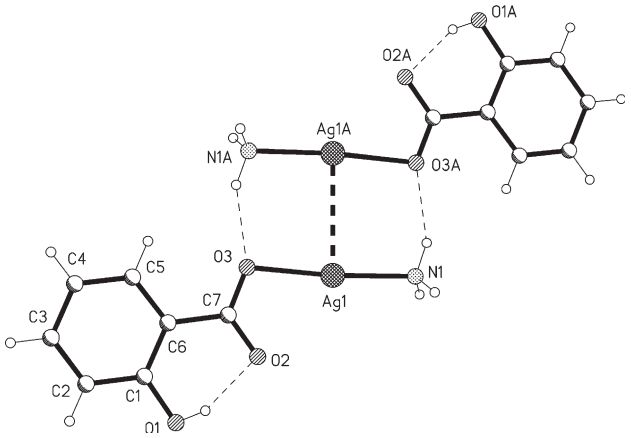

Fig. 1. X-ray crystal structure of $[Ag_2(NH_3)_2(salH)_2]$.

Table 1
Selected bond lengths (Å) and angles (°) for $[Ag_2(NH_3)_2(salH)_2]$

Ag(1)–N(1)	2.1367(17)
Ag(1)–O(3)	2.1699(14)
Ag(1)–O(2)	2.7577(14)
Ag(1)–Ag(1)#1	3.0685(4)
N(1)–Ag(1)–O(3)	175.37(5)
N(1)–Ag(1)–O(2)	132.88(5)
O(3)–Ag(1)–O(2)	51.74(4)
N(1)–Ag(1)–Ag(1)#1	90.47(4)
O(3)–Ag(1)–Ag(1)#1	84.90(4)
O(2)–Ag(1)–Ag(1)#1	136.62(3)

$SalH_2$, $[Ag_2(salH)_2]$ and $[Ag_2(NH_3)_2(salH)_2]$ were screened for their ability to inhibit the growth of *C. albicans* (Table 2). Whilst metal-free $salH_2$ was essentially ineffective at controlling the growth of the organism, $[Ag_2(salH)_2]$ did show quite marked activity. However, the ammonia complex $[Ag_2(NH_3)_2(salH)_2]$ displayed an approximately tenfold superior activity at controlling yeast cell proliferation. Previous investigations into the anti-microbial activity of $[Ag_2(salH)_2]$ suggested that its effects were due to the presence of free Ag^+ ions in a fashion similar to $AgNO_3$ [14]. Given the poorly water-soluble nature of $[Ag_2(salH)_2]$ (ca. 0.1 g per 100 cm^{-3} at pH 6.5) compared to $AgNO_3$ (250,000 mg per 100 cm^{-3} at pH 7), such a reasoning might be expected to account for the superior activity of $AgNO_3$ as the completely dissociated salt would give rise to a much higher concentration of free Ag^+ ions in the test media [14]. However, on a cautionary note, it must be emphasised that comparisons of solubilities of compounds in water with those in test media are likely to be unreliable given the multi-component nature of growth media. It must also be stressed that the present activity data cannot be rigorously interpreted to mean that the salicylate complexes remain intact throughout the screening protocol

Table 2
MIC data for *C. albicans*

Compound	MIC (μM)
$AgCH_3CO_2$ [1]	30
$AgNO_3$ [1]	30
$AgClO_4$ [1]	44
$salH_2$	>724
$[Ag_2(salH)_2]$	5.0
$[Ag_2(NH_3)_2(salH)_2]$	0.5

and that the MIC values reflect exactly the effects of either the free Ag^+ ion or the Ag(I) complexes. The small variations on the MIC values could result from common metabolites for the free metal ion and the complexes, which might be generated after incorporation into the cells. Either, metabolism of the complexes leading to free Ag^+ ion, or complexation of Ag^+ and ligand displacement of the $salH^-$ and NH_3 by a higher affinity ligand, extra- or intra-cellularly, could lead to the common results. It seems likely that the ammonia ligands in $[Ag_2(NH_3)_2(salH)_2]$ are in some way responsible for the superior activity of this complex compared to that of $[Ag_2(salH)_2]$, which does not have any coordinated NH_3. It is noteworthy that the inhibitory effect of $[Ag_2(NH_3)_2(salH)_2]$ is on a parity with that of the extremely active complex $[Ag(phendio)_2]ClO_4$ [1].

Previous studies on the mode of action of Ag(I) complexes have revealed that their anti-fungal activity is mediated though disruption of mitochondrial function [3]. For example, exposure of *C. albicans* to $[Ag_2(phen)_3(mal)]\cdot 2H_2O$ (phen = 1,10-phenanthroline; mal = malonic acid dianion) leads to a reduction in respiration with a concomitant depletion in the quantity of ergosterol in the fungal cell membrane. Ergosterol synthesis is disrupted because a depletion in respiration leads to a loss in NADH–NADPH cycling, which is required for the action of one of the enzymes in ergosterol biosynthesis [15]. The adverse effect on respiration appears to be due to the disruption of the synthesis of cytochromes (especially cytochrome aa3, components of which are mitochondrially encoded) [3]. Cytochromes form an integral part of the electron transfer pathway essential for aerobic respiration and consequently a reduction in their synthesis adversely affects respiration. In addition, Ag(I) complexes also induce apoptosis (programmed cell death) in fungal and mammalian cells which may be a direct result of their action on the cell or a secondary effect arising from their disruption of respiration. Cells treated with $[Ag_2(phen)_3(mal)]\cdot 2H_2O$ show extensive DNA fragmentation, mitochondrial disruption and retraction of the cytoplasm [16].

One feature of the $[Ag_2(phen)_3(mal)]\cdot 2H_2O$-mediated reduction in respiration and ergosterol synthesis is that this renders cells more tolerant of the polyene anti-fungal prescription drug amphotericin B [17]. Amphotericin B is one of the principal anti-fungal drugs used for the treatment of systemic, life-threatening mycoses and functions by binding to ergosterol in the cell membrane and creating pores through which intracellular constituents escape [18,19]. The reduced level of ergosterol in treated cells leads to a higher tolerance to this anti-fungal drug and may have implications for the treatment of fungal infections.

Ag(I) complexes demonstrate strong anti-fungal properties and appear to target the mitochondrion. This has the effect of reducing the amount of ergosterol in the cell membrane and may also trigger the process of apoptosis. Thus, such complexes may have therapeutic potential for the treatment of superficial fungal infections and they manifest a mode of action distinct to that of the conventional anti-fungal drugs [20] making them potentially applicable in situations where resistance to these prescription drugs has emerged to compromise therapy [21].

The chemotherapeutic potential of $salH_2$, $AgClO_4$ and the two salicylate complexes, $[Ag_2(salH)_2]$ and $[Ag_2(NH_3)_2(salH)_2]$, was determined against the three human derived cancer cell lines, Cal-27, Hep-G2 and A-498. Profiles of cell viability against drug concentration were established (Figs. 2–4) from which IC_{50} values were

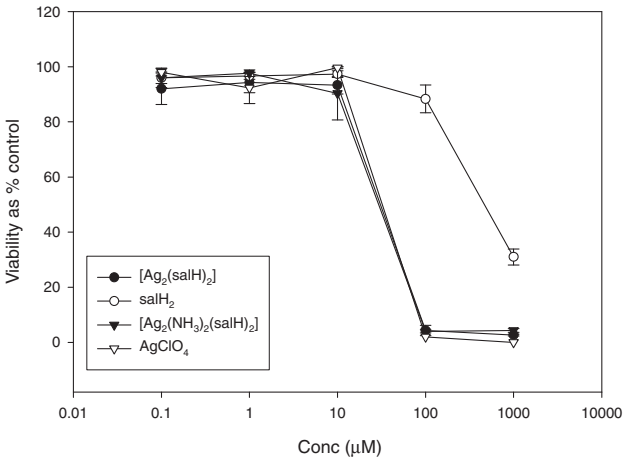

Fig. 2. Effects of $salH_2$, $[Ag_2(salH)_2]$, $[Ag_2(NH_3)_2(salH)_2]$ and $AgClO_4$ on the viability of Cal-27 cancer cells following continuous incubation with increasing drug concentration (0.1–1000 μM) for 96 h. Bars indicate standard error of the mean (SEM) and results were statistically significant from control at $p < 0.05$.

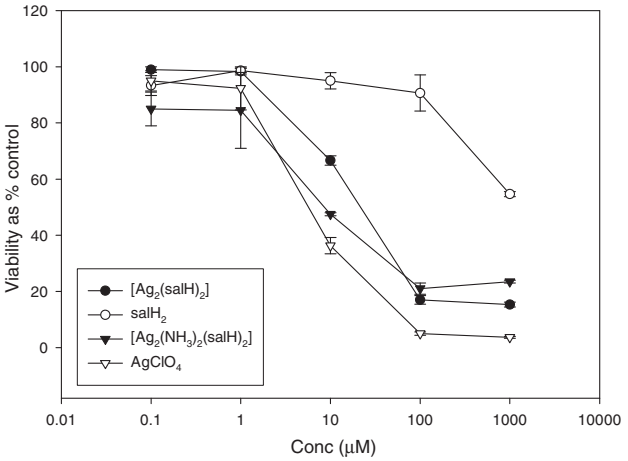

Fig. 3. Effects of $salH_2$, $[Ag_2(salH)_2]$, $[Ag_2(NH_3)_2(salH)_2]$ and $AgClO_4$ on the viability of Hep-G2 cancer cells following continuous incubation with increasing drug concentration (0.1–1000 μM) for 96 h. Bars indicate standard error of the mean (SEM) and results were statistically significant from control at $p < 0.05$.

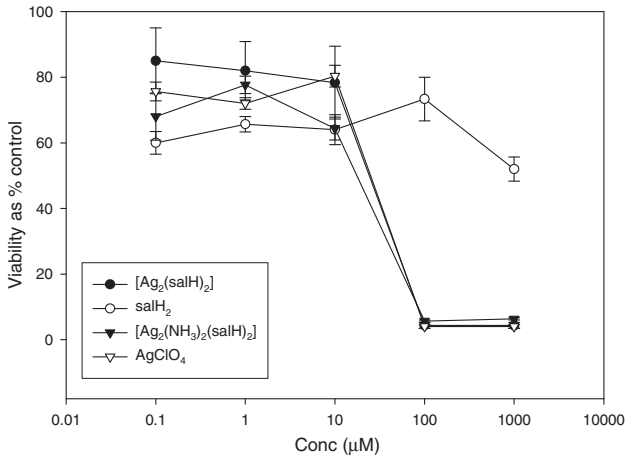

Fig. 4. Effects of $salH_2$, $[Ag_2(salH)_2]$, $[Ag_2(NH_3)_2(salH)_2]$ and $AgClO_4$ on the viability of A-498 cancer cells following continuous incubation with increasing drug concentration (0.1–1000 μM) for 96 h. Bars indicate standard error of the mean (SEM) and results were statistically significant from control at $p < 0.05$.

Table 3
IC_{50} values (μM) (mean ± SEM, $n = 5$) for compounds against Cal-27, Hep-G2 and A-498 cancer cells

Compound	Toxicities (IC_{50} μM)		
	Cal-27	Hep-G2	A-498
$salH_2$	700 ± 40	1000 ± 0	900 ± 141
$AgClO_4$	56 ± 0	8 ± 1	45 ± 2
$[Ag_2(salH)_2]$	27 ± 2	20 ± 1	18 ± 2
$[Ag_2(NH_3)_2(salH)_2]$	51 ± 11	9 ± 0	32 ± 7

calculated (Table 3). For all cell lines a concentration-dependent cytotoxic response was observed for all compounds. Whilst the metal-free carboxylic acid $salH_2$ had a mild cytotoxic effect across the three cell lines, the Ag(I)-containing species, $AgClO_4$, $[Ag_2(salH)_2]$ and $[Ag_2(NH_3)_2(salH)_2]$, were all highly toxic. However, this apparent Ag-related cytoxic effect is significant at drug concentrations greater than 10 μM, and in all of the cell lines studied. Close similarities were found in the viability versus concentration profiles for $AgClO_4$, $[Ag_2(salH)_2]$ and $[Ag_2(NH_3)_2(salH)_2]$ across all three cell lines (Figs. 2–4). Whilst there is no discrimination in the activity of $[Ag_2(salH)_2]$ across the three cell lines, both $AgClO_4$ and $[Ag_2(NH_3)_2(salH)_2]$ offer some bias towards inhibiting the growth of Hep-G2 cells.

3. Experimental

Chemicals, cell culture reagents and media were purchased from commercial sources and were used without further purification. $[Ag_2(salH)_2]$ was prepared in accordance with the literature procedure [4–6]. Infrared spectra of solids (in a KBr matrix) were recorded in the region 4000–400 cm^{-1} on a Nicolet FT-IR Impact 400D infrared spectrometer and ^1H NMR spectra were run on a Bruker Avance 300 MHz instrument. Microanalytical data were provided by the Microanalytical Laboratory, National University of Ireland, Cork, Ireland.

C. albicans ATCC 10231 was obtained form the American Type Culture Collection, (Manasas, VA, USA). Cultures were grown on Sabouraud dextrose agar (SDA) plates at 37 °C and maintained at 4 °C for short-term storage. Cultures were routinely sub-cultured every 4–6 weeks. Cultures were grown to the stationary phase (approximately 1×10^8 cells cm^{-3}) overnight at 30 °C and 200 rpm in minimal medium (MM) (2% w/v glucose, 0.5% w/v yeast nitrogen base (without amino acids or ammonium sulphate), 0.5% w/v ammonium sulphate). Solutions of water-soluble test salts were prepared by dissolving the salt (0.02 g) in distilled water (100 cm^3) to yield a stock solution with a concentration of 200 μg cm^{-3}. Doubling dilutions of this stock solution were made to yield a series of test solutions. The water-insoluble Ag(I) complexes, $[Ag_2(salH)_2]$ and $[Ag_2(NH_3)_2(salH)_2]$, were made up as suspensions (0.02 g) in water (100 cm^3) to give stock suspensions. With vigorous agitation of these suspensions doubling dilutions were made to give a series of test suspensions. Minimum inhibitory concentrations (MICs) were then determined using the broth microdilution method [2,3].

Cytotoxicity assays were performed using three human malignant model cell lines in order to assess the cancer chemotherapeutic potential of metal free Sal and its metal complexes. Therefore, squamous carcinoma tongue (Cal-27), hepatocellular carcinoma (Hep-G2) and kidney adenocarcinoma (A-496) cell lines were purchased from the ATCC. All cell lines were grown as monolayers in Eagle's minimum essential medium, supplemented with 2 mM L-glutamine and Earle's balanced salt solution, containing 1.5 g dm^{-3} sodium bicarbonate, 0.1 mM non-essential amino acids, 1.0 mM sodium pyruvate, 100 U cm^{-3} penicillin and 100 μg cm^{-3} streptomycin supplemented to contain 10% (v/v) foetal bovine serum (Flow laboratories, Herts, UK). All cells were grown at 37 °C in a humidified atmosphere, in the presence of 5% CO_2 and were in the exponential phase of growth at the time of assay. Cytotoxicity was assessed using the MTT assay. Each of the three cell lines (100 μl) were seeded at a density of 5×10^4 cells cm^{-3} into sterile 96-well flat-bottomed plates (Falcon Plastics, Becton Dickinson) and grown in 5% CO_2 at 37 °C. Test compounds were dissolved in DMSO and diluted with culture media. The maximum percentage of DMSO present in all wells was 0.2% (v/v). Each drug solution (100 μl) was added to replicate wells in the concentration range of 0.1–1000 μM and incubated for 96 h. A miniaturised viability assay using 3-(4,5-dimethylthiazol-2-yl)-2,5-diphenyl tetrazolium bromide (MTT) was carried out ac-

cording to the method described by [22]. The IC_{50} value, defined as the drug concentration causing a 50% reduction in cellular viability, was calculated for each drug. Each assay was carried out using five replicates and repeated on at least three separate occasions. Viability was calculated as a percentage of solvent-treated control cells and expressed as a percent (%) of the control. The significance of any reduction in cellular viability was determined using one-way ANOVA (analysis of variance). A probability of 0.05 or less was deemed statistically significant.

4. $[Ag_2(NH_3)_2(salH)_2]$

The following procedure was conducted with the exclusion of light. To a suspension of Ag_2O (0.5 g, 2.0 mmol) in water (10 cm^3) was added, dropwise, concentrated aqueous NH_3 until all solid had dissolved. Salicylic acid ($salH_2$) (0.55 g, 4.0 mmol) was added and the solution stirred at room temperature for 0.5 h. The solution was evaporated to dryness and the grey solid resuspended in ethanol (5 cm^3). The solid was filtered off, washed with small portions of chilled water, ethanol and ether and then air-dried. Yield: 0.83 g (79%). The sample was stored with the exclusion of light. The sample was soluble in hot acetonitrile and in DMSO, and was essentially insoluble in water. *Anal.* Calc.: C, 32.25; H, 3.08; N, 5.34%. Found: C, 32.23; H, 3.02; N, 5.05. IR (KBr): 3457, 3235, 2927, 1646, 1596, 1492, 1461, 1393, 1338, 1301, 1252, 1153, 1030, 861, 812, 750, 701, 670, 535 cm^{-1}. ^1H NMR (ppm DMSO): 14.47 (s, 1H, OH), 7.78 (d, 1H, phenyl ring), 7.24 (t, 1H, phenyl ring), 6.71 (m, 2H, phenyl ring), 3.01 (s, 3H, NH_3). Crystals suitable for X-ray analysis were obtained following recrystallisation from hot acetonitrile.

4.1. X-ray crystallography

Crystal data for $[Ag_2(NH_3)_2(salH)_2]$ were collected at 150(2) K on a Bruker SMART 1000 diffractometer. The structure was solved by direct methods and refined by full-matrix least-squares on F^2 using the SHELXTL suite of programs [23]. All non-hydrogen atoms were refined with anisotropic atomic displacement parameters. Hydrogen atoms were inserted at calculated positions using a riding model except for the phenolic proton, which was located from difference maps and allowed to refine with a fixed atomic displacement parameter. Details of the data collection and structure refinement are given in Table 4.

Supplementary data for $[Ag_2(NH_3)_2(salH)_2]$ are available from the Cambridge Crystallographic Data Centre, 12 Union Road, Cambridge CB2 1EZ, England (Fax: +44-1223-336033), on request quoting the deposition number CCDC 224787.

Table 4
Crystal data and structure refinement for $[Ag_2(NH_3)_2(salH)_2]$

Empirical formula	$C_{14}H_{16}Ag_2N_2O_6$
Formula weight	524.03
Temperature (K)	150(2)
Wavelength (Å)	0.71073
Crystal system	Monoclinic
Space group	$P2(1)/n$
Unit cell dimensions	
a (Å)	7.0807(6)
b (Å)	7.1443(6)
c (Å)	15.7625(14)
α (°)	90
β (°)	94.361(2)
γ (°)	90
Volume (Å^3)	795.06(12)
Z	2
Density (calculated) (Mg/m^3)	2.189
Absorption coefficient (mm^{-1})	2.497
$F(000)$	512
Crystal size (mm^3)	$0.33 \times 0.09 \times 0.08$
Crystal description	Colourless rod
Theta range for data collection	2.59–28.74°
Index ranges	$-9<=h<=9$, $-9<=k<=9$, $-21<=l<=20$
Reflections collected	6537
Independent reflections	1886 [$R_{int} = 0.0157$]
Completeness to theta = 26.00°	99.9%
Absorption correction	Semi-empirical from equivalents
Maximum and minimum transmission	1.00000 and 0.761510
Refinement method	Full-matrix least-squares on F^2
Data/restraints/parameters	1886/0/113
Goodness-of-fit on F^2	1.040
Final R indices [$I > 2\sigma(I)$]	$R_1 = 0.0171, wR_2 = 0.0403$
R indices (all data)	$R_1 = 0.0202, wR_2 = 0.0413$
Largest differential peak and hole	0.312 and −0.399 e Å^{-3}

Acknowledgements

This research was funded, in part, by The Technological Sector Research Scheme, Strand III (2000–2006). B. Coyle acknowledges financial support from Enterprise Ireland.

References

[1] M. McCann, B. Coyle, S. McKay, P. McCormack, K. Kavanagh, M. Devereux, V. McKee, P. Kinsella, R. O'Connor, M. Clynes, BioMetals (in press).
[2] M. McCann, M. Geraghty, M. Devereux, D. O'Shea, J. Mason, L. O'Sullivan, Metal-Based Drugs 7 (2000) 185–193.
[3] B. Coyle, K. Kavanagh, M. McCann, M. Devereux, M. Geraghty, BioMetals 16 (2003) 321–329.
[4] T.C.W. Mak, W.-H. Yip, C.H.L. Kennard, G. Smith, E.J. O'Reilly, Aust. J. Chem. 39 (1986) 541–546.
[5] G. Smith, C.H.L. Kennard, T.C.W. Mak, Z. Kristallogr. 184 (1988) 275–280.
[6] E.M. Movsumov, A.S. Antsyshkina, V.N. Ostrikova, K.T. Karaeva, M.A. Porai-Koshits, Koord. Khim. (Russ.) (Coord. Chem.) 16 (1990) 517–520.

[7] S.-L. Zheng, M.-L. Tong, H.-L. Zhu, X.-M. Chen, New J. Chem. 25 (2001) 1425–1429.
[8] C. Hollatz, A. Schier, H. Schmidbaur, J. Am. Chem. Soc. 119 (1997) 8115–8116.
[9] B.T. Usubaliev, É.M. Movsumov, I.R. Amiraslanov, A.I. Akhmedov, A.A. Musaev, K.S. Mamedov, J. Struct. Chem. 22 (1981) 73–77.
[10] A. Bayler, A. Schier, G.A. Bowmaker, H. Schmidbaur, J. Am. Chem. Soc. 118 (1996) 7006–7007.
[11] A. Dedieu, R. Hoffmann, J. Am. Chem. Soc. 100 (1978) 2074–2079.
[12] P. Pyykkö, Chem. Rev. 97 (1997) 597–636.
[13] H. Schmidbaur, Gold Bull. (Lond.) 33 (2000) 3–10.
[14] A. Bult, B.L. Bajema, H.B. Klasen, H.J. Meeting, C.L. Fox Jr., Pharm. Weekblad Sci. Edn. 3 (1981) 79–81.
[15] L.W. Parks, W.M. Casey, Ann. Rev. Microbiol. 49 (1995) 95–116.
[16] B. Coyle, P. Kinsella, M. McCann, M. Devereux, R. O'Connor, M. Clynes, K. Kavanagh, Toxicol. in Vitro 18 (2004) 63–70.
[17] A. Eshwika, B.Coyle, M. Devereux, M. McCann, K. Kavanagh, BioMetals (in press).
[18] K.M. Abu-Salah, Brit. J. Biomed. Sci. 53 (1996) 122–133.
[19] S. Hartsel, J. Bolard, TIPS 17 (1996) 445–449.
[20] T.C. White, K.A. Marr, R.A. Bowden, Clin. Microbiol. Rev. 11 (1998) 382–402.
[21] M. Canuto, F.G. Rodero, Lancet (Infect. Dis.) 2 (2002) 550–562.
[22] T. Mosmann, J. Immunol. 65 (1983) 55–63.
[23] G.M. Sheldrick, SHELXTL Version 5.1, Bruker AXS, Madison, Wisconsin, USA, 1998.